Hindawi Publishing Corporation
Journal of Nanomaterials
Volume 2013, Article ID 536291, 9 pages
http://dx.doi.org/10.1155/2013/536291

Research Article

Bovine Serum Albumin-Loaded Chitosan/Dextran Nanoparticles: Preparation and Evaluation of *Ex Vivo* Colloidal Stability in Serum

Haliza Katas, Zahid Hussain, and Siti Asarida Awang

Centre for Drug Delivery Research, Faculty of Pharmacy, Universiti Kebangsaan Malaysia, Kuala Lumpur Campus, Jalan Raja Muda Abdul Aziz, 50300 Kuala Lumpur, Malaysia

Correspondence should be addressed to Haliza Katas; haliz12@hotmail.com

Received 1 January 2013; Revised 22 March 2013; Accepted 7 April 2013

Academic Editor: Xing-Jie Liang

Copyright © 2013 Haliza Katas et al. This is an open access article distributed under the Creative Commons Attribution License, which permits unrestricted use, distribution, and reproduction in any medium, provided the original work is properly cited.

Chitosan (CS) nanoparticles have several distinct intrinsic advantages; however, their *in vivo* colloidal stability in biological fluids was not fully explored especially when carrying proteins. The present study aimed to investigate their colloidal stability using an *ex vivo* physiological model of fetal bovine serum (FBS) and human serum (HS). The stability of bovine-serum-albumin (BSA-) loaded nanoparticles was relatively higher in FBS than that in HS. Particle size of unloaded and BSA-loaded nanoparticles was statistically unchanged up to 24 h after incubation in FBS. However in HS, a significant increase in particle size from 144 ± 17 to 711 ± 22 nm was observed for unloaded nanoparticles and by 2.5-fold for BSA-loaded nanoparticle, at 24 h after incubation in HS. Zeta potential of both nanoparticles was less affected by the components in FBS compared to those in HS. A remarkable swelling extent was experienced for unloaded and BSA-loaded nanoparticles in HS, up to 54 ± 4% and 44 ± 5%, respectively. Morphology of unloaded and BSA-loaded nanoparticles was varied from smooth spherical and rod shape to irregular shape when incubated in FBS; however, form agglomerates when incubated in HS. These findings therefore suggest that HS is more reactive to cause colloidal instability to the chitosan nanoparticles compared to FBS.

1. Introduction

Despite several intrinsic and distinct advantages of nanoparticles, the concerns about the health risks of polymeric nanoparticles have been escalating nowadays due to the higher incidence of instability of nanoformulations. Numerous *in vitro* studies reported that the nanosized particles are biologically more potent than the equivalent micron-sized particles of same chemical composition [1, 2]. The potency and biological activity of polymeric nanoparticles have been connected with several physicochemical (colloidal) characteristics such as the shape of the particles, their surface area, hydrodynamic particle size, agglomeration or flocculation rate, surface potential (zeta potential), and the surface chemistry of nanoparticles [3]. These physicochemical characteristics of polymeric nanoparticles are in turn highly affected by the medium in contact such as biological fluids (plasma, serum, saliva, sweat, sebum, tears, etc.). Thus, it was argued that the physicochemical properties and unique kinetics of nanomaterials in biological solutions should be considered prior to various pharmaceutical and pharmacodynamic testings [3–5]. Besides, the adsorption and desorption affinities of reactive components of biological fluids (such as proteins) onto the nanoparticles surface, type, amount, and conformation of the adsorbed proteins are necessary to be considered when analyzing the biological responses of the nanoparticles [6, 7].

Among the biological fluids, fetal bovine serum (FBS), a commonly used supplement for cell culture, and the human serum (HS), the main component of human blood [8], were used in the current research to assess the colloidal stability of nanoparticles. Serum is a complex mixture of different factors and contains a large number of components like growth factors, proteins, vitamins, hormones, trace elements, and other essential and nonessential components [9]. Serum

components would tend to alter the colloidal characteristics (particle size, PDI, and zeta potential) of polymeric nanoparticles and carry their own surface charges (e.g. proteins with negative charges while some growth hormones exhibit positive charges) which may influence the overall physicochemical characteristics of polymeric nanoparticles [10, 11]. Therefore, determination of protein stability in serum constitutes a powerful and important screening assay. *In vivo* testing of peptide stability is obviously of more relevance than *in vitro* but blood samples should be as steriled as possible to ensure maximum activity of proteolytic enzymes and minimal interference with the assay [12]. Besides that the blood is a biohazardous material, it must also be heparinised and this may interfere with the assay.

Recently, for preparing the polymeric nanoparticles, chitosan (CS) has been extensively focused on. CS is a natural biopolymer derived from chitin deacetylation [13, 14]. It has attained a remarkable attention due to its biological properties such as excellent biocompatibility, hydrophilicity, biodegradability, and antibacterial activity [15]. Gan and Wang [16] had recommended the CS as the superior particulate polymer for *in vivo* administration due to its nontoxic nature and degradation by the action of lysozyme in the body. Besides, CS is a good candidate for *in vivo* and *ex vivo* applications because it would not accumulate in body tissues [17].

Taken together, the selection of cross-linking agent used in the particle preparation is also an imperative factor to further improve the colloidal stability of CS nanoparticles. Thus, in the present study, CS nanoparticles were prepared by ionic-cross linking of CS with dextran sulphate (DS). The criterion for using DS as the cross-linking agent is that it had been reported to produce mechanically more stable nanoparticles compared to the penta-sodium tripolyphosphate (TPP) [18, 19]. Moreover, CS/DS nanoparticles offer many therapeutic advantages over CS/TPP nanoparticles. Particle size of CS/DS nanoparticles was comparatively small which directly affect the colloidal stability of particulate dispersion [20]. Besides the particle size, zeta potential is also the vital indicator to predict and control the stability of colloidal dispersion [21]. Hence, the present study was aimed to investigate the colloidal stability of CS/DS nanoparticles in HS and FBS. The colloidal stability was assessed in terms of particle size, zeta potential, PDI, swelling characteristics, and as well as the morphology of CS/DS nanoparticles.

2. Materials and Methods

2.1. Materials. Low molecular weight chitosan (deacetylation degree, 75–85%, M.wt, 70 kDa), glacial acetic acid (CH_3COOH), dextran sulphate (DS), bovine serum albumin (BSA) (M.wt, 46 kDa), Bradford reagent, fetal bovine serum, and human serum (obtained from human male AB plasma) were purchased from Sigma-Aldrich, USA. All other chemicals were of analytical grades and used without further purification.

2.2. Preparation of Unloaded CS/DS Nanoparticles. CS/DS nanoparticles were prepared *via* ionic-gelation method, previously developed by Calvo et al. [26] with some modification. CS was dissolved in 1% v/v glacial acetic acid to produce 0.075% w/v CS solution. Three different concentrations of DS (0.075, 0.1, and 0.125% w/v) were prepared by dissolving DS in distilled water. CS/DS nanoparticles were prepared simultaneously by adding 40 mL of DS solution dropwise in 100 mL of 0.075% w/v CS solution under a constant magnetic stirring at 700 rpm for 30 min. Thereafter, CS/DS nanoparticles were harvested by ultracentrifugation (25000 rpm) using an Optima L-100 XP Ultracentrifuge (Beckman-Coulter, USA) with a rotor NV 70.1 Ti (Beckman-Coulter, USA) at 10°C for 15 min.

2.3. Preparation of BSA-Loaded CS/DS Nanoparticles. For preparing BSA-loaded CS/DS nanoparticles, BSA was dissolved in PBS solution (pH, 7.4) to produce the concentration of 1 mg/mL. The pH of CS solution was then adjusted to 5.5 by adding either 0.5 M NaOH or 0.5 M HCl. BSA solution was then premixed with 0.075% w/v CS solution and incubated for 30 min at room temperature. DS solution (0.075, 0.1 and 0.125% w/v) was then added dropwise in the reaction mixture under a continuous magnetic stirring (700 rpm) for 30 min to produce BSA-loaded CS/DS nanoparticles. The resultant nanoparticles were harvested by ultracentrifugation at 25000 rpm at 10°C for 15 min.

2.4. Determination of Particle Size, PDI, and Zeta Potential. Mean particle size, PDI, and zeta potential of unloaded and BSA-loaded CS/DS nanoparticles were measured by using a ZS-90 Zetasizer (Malvern Instruments, UK). For particle size analysis, measurements were performed at 25°C with a detection angle of 90°. All measurements were performed in triplicate and results were reported as mean ± standard deviation (S.D).

2.5. Entrapment Efficiency (EE). To determine EE, the BSA-loaded CS/DS nanoparticles were harvested by ultracentrifugation at 25000 rpm using Optima L-100 XP Ultracentrifuge (Beckman-Coulter, USA) with a rotor NV 70.1 Ti (Beckman-Coulter, USA) at 10°C for 15 min. Supernatants recovered by ultra-centrifugation were then decanted, and the BSA contents were analyzed using Bradford protein assay as per manufacturer's instructions. The samples were then subjected to U.V/Vis spectrophotometer (U.V-1601, Shimadzu, Japan) and analyzed at 595 nm (λ_{max}), and U.V absorbance was recorded. The percent EE of BSA was then calculated indirectly from remaining supernatant using the following equation [22]:

$$\begin{aligned} \text{EE} = {} & (\text{Total initial amount of BSA added} \\ & - \text{Free amount of BSA in supernatant}) \\ & \times (\text{Total initial amount of BSA added})^{-1} \\ & \times 100 \end{aligned} \quad (1)$$

2.6. Stability Studies of CS/DS Nanoparticles in Serum. To assess the colloidal stability of unloaded and BSA-loaded CS/DS nanoparticles, FBS was first incubated at 37°C in a water bath incubator to simulate physiological media. FBS was then added in the CS/DS nanoparticles dispersion with the volume ratio of 1 : 1 in which the final concentration of 50% v/v of serum was yielded. Subsequently, the resulting mixture was incubated in the water bath incubator at 37°C for 24 h. The mean particle size, PDI, and surface charge were measured at predetermined time points (0, 10, 30 min, 1, 2, 3, 12, and 24 h). Same experimental protocol was also repeated to determine the colloidal stability of CS/DS nanoparticles in HS. CS/DS nanoparticles were suspended in PBS (pH, 7.4) prior to mixing with FBS or HS.

2.7. Swelling Analysis. To investigate the swelling characteristics of CS/DS nanoparticles, 100 mg of lyophilized powder sample of either unloaded or BSA-loaded CS/DS nanoparticles was immersed in 100 mL of FBS and/or HS at various DS concentrations (0.075, 0.1, and 0.125) for 24 h at room temperature until a swollen equilibrium was achieved. The swollen samples were then collected by filtration, blotted with filter paper for the removal of the surface adsorbed water, and weighed immediately. Then, the swelling ratios of CS/DS nanoparticles were calculated using the following equation [23]:

$$\text{Swelling ratio } (\%) = \left(W_s - \frac{W_d}{W_d}\right) \times 100, \quad (2)$$

where W_s and W_d are the average weights of swollen and dry samples, respectively. Results were reported as mean ± S.D.

2.8. Morphological Examination. With a view to evaluate the effect of FBS and HS on the morphological characteristics of CS/DS nanoparticles, the unloaded and BSA-loaded nanoparticles were incubated in both sera for 24 h and were viewed under transmission electron microscope (TEM). Prior to TEM analysis, the incubated dispersions of CS/DS nanoparticles (in FBS or HS at 24 h after incubation) were diluted to 1 : 10 ratio with phosphate buffered saline (PBS, 0.01 M). The resulting dilution was carried out in order to obtain the clear images (microscopic micrographs) of CS/DS nanoparticles under TEM. To perform the microscopic (TEM) analysis, a drop of diluted nanoparticles dispersion in FBS or HS was placed onto the copper microgrid that was natively stained with phosphotungstic acid and allowed to evaporate and dry at room temperature (25 ± 2°C). The dried microgrids were then viewed at different TEM resolutions to assess the morphology of unloaded and BSA-loaded nanoparticles before and after incubation in FBS and HS.

2.9. Statistical Analysis. The data was presented as mean ± standard deviation (S.D). Data was analyzed using SPSS 17.0 (paired t-test and independent t-test and ANOVA, followed by Tukey's post hoc analysis). For paired t-test, $P < 0.05$ showed the significant difference between the mean of tested groups. For independent t-test, $P < 0.05$ showed significant difference between the mean of two independent tested samples.

3. Results and Discussion

3.1. Colloidal Characteristics of CS/DS Nanoparticles

3.1.1. Particle Size, PDI, and Zeta Potential. Figures 1(a) and 1(b) present the results of particle size and zeta potential of unloaded and BSA-loaded CS/DS nanoparticles prepared from different concentrations of DS (0.075, 0.1, 0.125% w/v). Data clearly demonstrates that the particle size and zeta potential of CS/DS nanoparticles were not significantly affected by the DS concentrations ($P > 0.05$, ANOVA, Tukey's post-hoc analysis), regardless of unloaded or BSA-loaded nanoparticles. The results obtained were different from the previously published results [24]. In present study, DS concentrations had less impact on the particle size, PDI, and zeta potential of CS/DS nanoparticles. This was expected because CS/DS weight ratio of different formulations was small and therefore yielded nanoparticles with almost similar colloidal characteristics. The CS/DS weight ratios studied in the present study were 1 : 1, 1 : 1.3, and 1 : 1.7 for 0.075, 0.1, and 0.125% w/v DS, respectively, while, the weight ratios of 5 : 3, 5 : 5, 5 : 10, and 5 : 20 were applied in the previous report. Despite that, all the formulations were within the nanosized range (200~300 nm). On the other hand, the lower surface charges of BSA-loaded CS/DS nanoparticles as compared to the unloaded nanoparticles were expected to be due to the neutralization of positive charges ($-NH_3^+$) on the contour of CS by the negatively charged BSA molecules [22, 24, 25], and this resulted in a decrease of the overall surface charge of nanoparticles as shown in Figure 1(b).

3.1.2. Entrapment Efficiency (EE). Data revealed that the EE of BSA was observed to be affected by the DS concentrations. A higher EE was obtained when the CS/DS weight ratio was reduced. The lowest CS/DS weight ratio (1 : 1) produced nanoparticles with the highest EE (95 ± 2%) of BSA. EE for the other DS concentrations wase found to be 91 ± 2% (at 1 : 1.3) and 86 ± 2% (at 1 : 1.7). This was expected as increase in the concentration of DS that would tend to increase the negative charge density on the surface of nanoparticles which may subsequently increase the repulsion energy against the negatively charged BSA molecules which might not be favourable for the protein entrapment process.

Furthermore, EE of BSA was also affected by pH of CS solution. The optimal pH was found to be at 5.5. The highest EE achieved in this study without adjusting the pH of CS solution to 5.5 was only 46 ± 4% (CS/DS weight ratio 1 : 1). This finding was in agreement with Calvo et al. [26] which reported that the greatest loading efficiency could be obtained when protein was dissolved at a pH above its isoelectric point (pH 4.8). At this pH, BSA would predominantly exhibit its highest negative charge and could ionically interact with positively charged $-NH_3^+$ groups on the backbone of CS. BSA also tends to be more negative as the pH of media

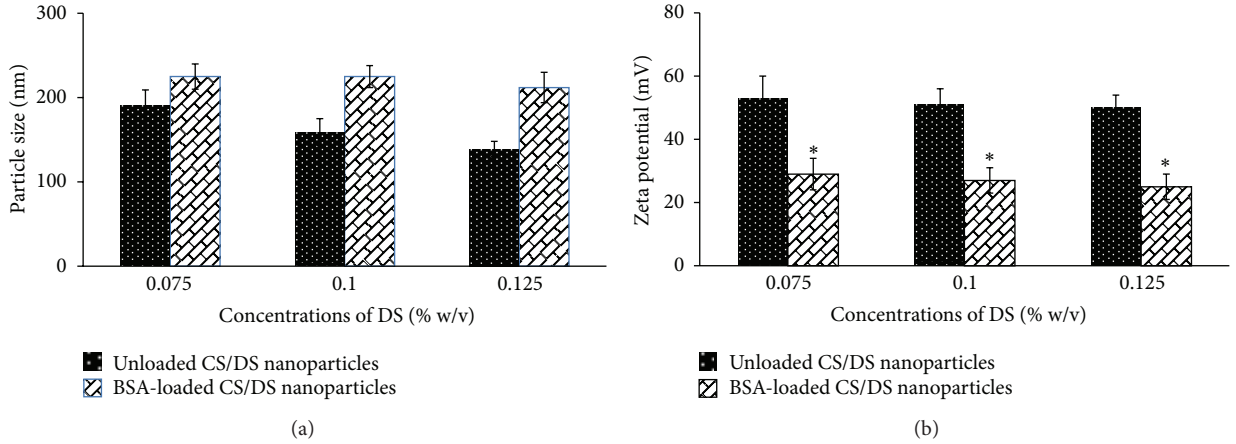

Figure 1: Particle size and zeta potential of unloaded and BSA-loaded CS/DS nanoparticles at various concentrations of DS (CS 0.075% w/v, BSA 1 mg/mL, 37°C, mean ± S.D, $n = 3$). *Particle surface charge of BSA-loaded was significantly different from unloaded CS/DS nanoparticles.

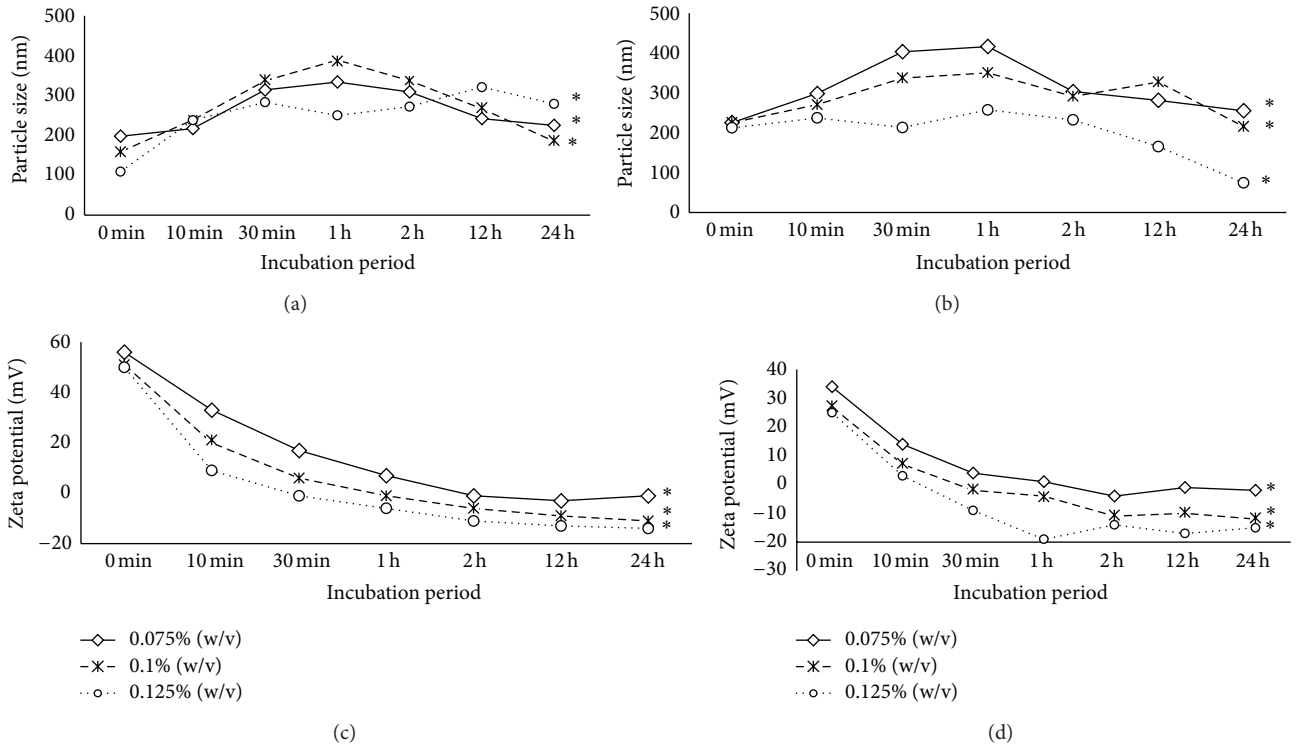

Figure 2: Particle size of unloaded (a) and BSA-loaded (b) and zeta potential of unloaded (c) and BSA-loaded (d) CS/DS nanoparticles at various concentrations of DS when incubated in FBS (CS 0.075% w/v, BSA 1 mg/mL, mean ± S.D, $n = 3$). *Significantly different from before incubation in serum.

increases above its isoelectric point [27] which favours the entrapment of BSA into the CS nanoparticles.

3.2. Colloidal Stability of CS/DS Nanoparticles

3.2.1. Stability in FBS. Figures 2(a) and 2(b) clearly highlight that the particle size of both unloaded and BSA-loaded CS/DS nanoparticles (prepared from 0.075% w/v of DS) was significantly increased ($P < 0.05$, independent t-test) at 1 h after incubation and declined from this point, up to 24 h after incubation. Similarly, the zeta potential showed a significant decline ($P < 0.05$, independent t-test) from +56 ± 5 and +34 ± 4 mV to +33 ± 3 and +14 ± 2 mV for unloaded (Figure 2(c)) and BSA-loaded nanoparticles (Figure 2(d)), respectively, at 10 min after incubation in FBS. A further decrease in zeta potential of both nanoparticles was also observed over time and this was thought to be caused by their interactions

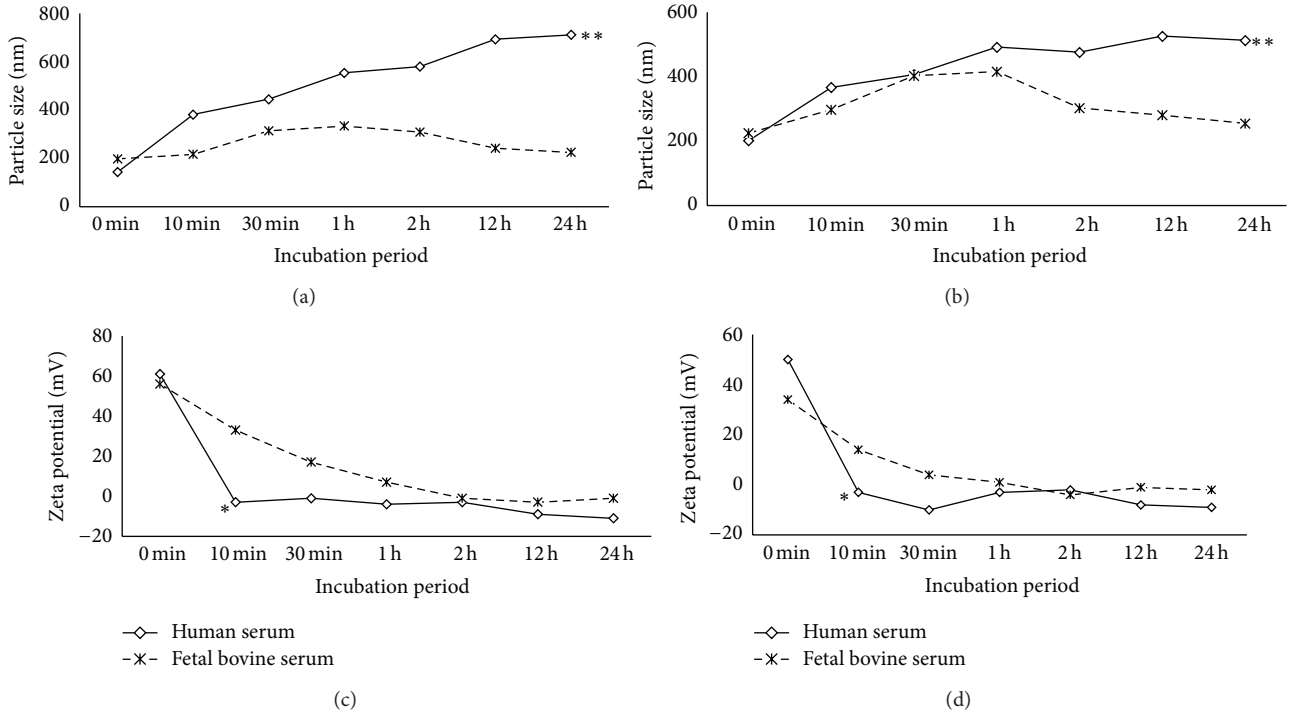

Figure 3: Particle size of unloaded (a), BSA-loaded (b), and zeta potential of unloaded (c) and BSA-loaded (d) CS/DS nanoparticles in HS and FBS (CS 0.075% w/v, BSA 1 mg/mL, mean ± S.D, $n = 3$). **Particle size of nanoparticles incubated in HS was significantly different from the ones before incubation and incubated in FBS. Particle surface charge of nanoparticles incubated in HS was significantly different from the ones before incubation and incubated in FBS.

with negatively charged albumin macromolecules (>−20 mV) in the incubation media. The obtained data also suggested that the unloaded nanoparticles were more strongly affected by the components in FBS than the BSA-loaded one. This might be due to stronger ionic interactions between serum albumin and the unloaded nanoparticles which had relatively higher positive surface charges as compared to BSA-loaded nanoparticles. The positive surface charge density of BSA-loaded CS/DS nanoparticles was relatively low due to the neutralization action by the BSA during the loading stage [28]. Moreover, charge neutralization by the albumin macromolecules in the incubating media further reduced repulsion energy between nanoparticles. This may also progressively facilitate agglomeration process and promote the formation of larger particles [9]. The tendency of particles to form aggregates was less prominent in case of BSA-loaded nanoparticles because they possessed relatively low zeta potential (positive charges) which subsequently resulted in a lesser degree of interaction with negatively charged components in FBS. Thus, this suggested that BSA-loaded nanoparticles had better colloidal stability in FBS compared to the unloaded ones. This finding is important because colloidal stability in serum for any nanoparticulate system determines the successful delivery of protein/peptides as it prevents particle aggregation or embolism from occurring in the systemic circulation [29].

The incubation time is also a critical factor to determine the adsorption pattern of proteins on the solid surfaces of nanoparticles [30]. In accordance to that, the particle size and zeta potential of unloaded and BSA-loaded nanoparticles were significantly influenced by the incubation time. Figure 2 clearly shows the changing patterns of the particle size and zeta potential over extended incubation time. A significant difference ($P < 0.05$, paired t-test) was observed among particle sizes at the different postincubation time points. For example, BSA-loaded CS/DS nanoparticles prepared from 0.075% w/v of DS were found to be enlarged from 225 ± 15 to 416 ± 21 nm at 1 h after incubation in FBS as shown in Figure 2(b). However, the particle size was subsequently decreased to 303 ± 18 nm at 2 h after incubation in FBS. This phenomenon could be explained by the process of association and dissociation of protein molecules on the surfaces of nanoparticles during the course of incubation. These results were also in accordance with previously published study that reported the adsorption, and desorption could also take place during *in vivo* circumstances [31]. Likewise, the continuous fluctuations of the nanoparticles zeta potential in response of continuous attraction-repulsion processes may indicate the positive and negative charge shifting between the particle surface and serum components in order to stabilize the nanoparticles in the serum medium as shown in Figure 2.

3.2.2. Stability in HS. For *in vivo* correlation, the stability analysis of unloaded and BSA-loaded CS/DS nanoparticles (produced from DS 0.075% w/v) was further carried out in the HS as presented in Figure 3. The selection of nanoparticles produced from DS 0.075% w/v was based on the criterion

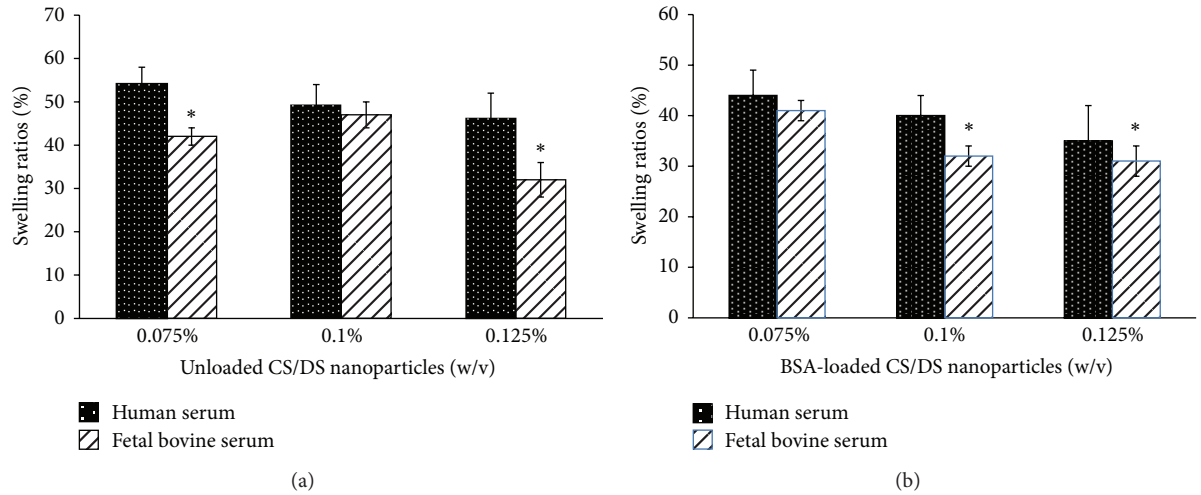

Figure 4: Swelling ratio of unloaded (a) and BSA-loaded (b) CS/DS nanoparticles in human and fetal bovine sera at various CS/DS weight ratios (CS 0.075% w/v, BSA 1 mg/mL, mean ± S.D, $n = 3$). *Significantly different from the nanoparticles incubated in HS.

that it was observed to be more stable in FBS with respect to its colloidal characteristics (particle size and zeta potential) as shown in Figure 3. The obtained data revealed that a significant increment ($P < 0.05$, paired t-test) in the particle size and zeta potential of unloaded and BSA-loaded nanoparticles occurred at 10 min after incubation in the HS. The particle size of unloaded and BSA-loaded nanoparticles was increased from 144 ± 17 and 202 ± 20 nm to 382 ± 21 and 367 ± 13 nm, respectively, at 10 min after incubation in HS. The increase in the particle size was expected to be due to the formation of particle aggregates due to an abrupt decline ($P < 0.05$, paired t-test) in the zeta potential of unloaded and BSA-loaded nanoparticles from +61 ± 6 and +50 ± 7 mV to −3 ± −0.2 and −3 ± −0.4 mV, respectively, after 10 min, incubation in HS. The particle size of unloaded and BSA-loaded nanoparticles was further increased to 711 ± 22 and 513 ± 21 nm at 24 h after incubation, respectively, when incubated in HS. Conversely, their zeta potential was not changed significantly ($P > 0.05$, paired t-test) from 10 min to 24 h after incubation as shown in Figures 3(c) and 3(d). However, a significant variation in the particle size and zeta potential of CS/DS nanoparticles regardless of unloaded or BSA-loaded type nanoparticles was expected to be in response of variable interaction between nanoparticles and protein components in HS.

Moreover, particle size of both unloaded and BSA-loaded CS/DS nanoparticles in FBS and HS was significantly increased ($P < 0.05$, independent t-test). However, the obtained data further revealed that both the unloaded and BSA-loaded nanoparticles had a higher tendency to form aggregate in HS compared to FBS as shown in Figures 3(a) and 3(b), respectively. For example, in HS, the particle size of BSA-loaded nanoparticles recorded at 1 h after incubation was 492 ± 24 nm, while, in FBS the particle size was 416 ± 21 nm at the same predetermined time point. Similarly, the largest particle size of unloaded nanoparticles in the HS (554 ± 26 nm) was observed to be higher than the one which obtained in the FBS (334 ± 15 nm) at 1 h after incubation. In addition, the surface charge of unloaded and BSA-loaded CS/DS nanoparticles declined at higher rate and extent in HS compared to FBS during the course of incubation as shown in Figures 3(c) and 3(d).

This diversity could be explained on the basis of disparity into the certain biological components that actively interact with unloaded and BSA-loaded CS/DS nanoparticles in both sera. According to Zelphati et al. [11], antibodies such as globulin and immunoglobulin are more likely abundant in the HS as compared to FBS. Furthermore, FBS is normally derived from calf in which the organ function and enzymes activity were not fully developed and thus resulted in diminished synthesis of antibodies. Meanwhile, the HS is normally sourced from adults in whom the organs and enzymes regulation are functioning optimally and contribute with promising potential to synthesize functional immunoglobulin and globulin.

3.3. Swelling Studies. Figure 4 shows the swelling characteristics of unloaded and BSA-loaded CS/DS nanoparticles in HS and FBS at various CS/DS weight ratios. Generally, the swelling ratio of unloaded and BSA-loaded CS/DS nanoparticles was less affected by the DS concentration. A higher swelling ratio for those nanoparticles prepared at the lowest weight ratio (1 : 1) was expected because high positive charges on the nanoparticles surfaces had provided more cross-linking sites available for bonding with surrounded water (water of hydration). These findings were also in accordance with the previously published data which reported that high surface charge facilitates the strong interaction with water of hydration [32]. The resulting interaction between polymer (CS) and water of hydration may facilitate the diffusion of water molecules into the polymer matrices and cause the nanoparticles to swell up. Besides that, a high positive zeta potential of CS/DS nanoparticles promotes a stronger intermolecular electrostatic repulsion which compels the polymer

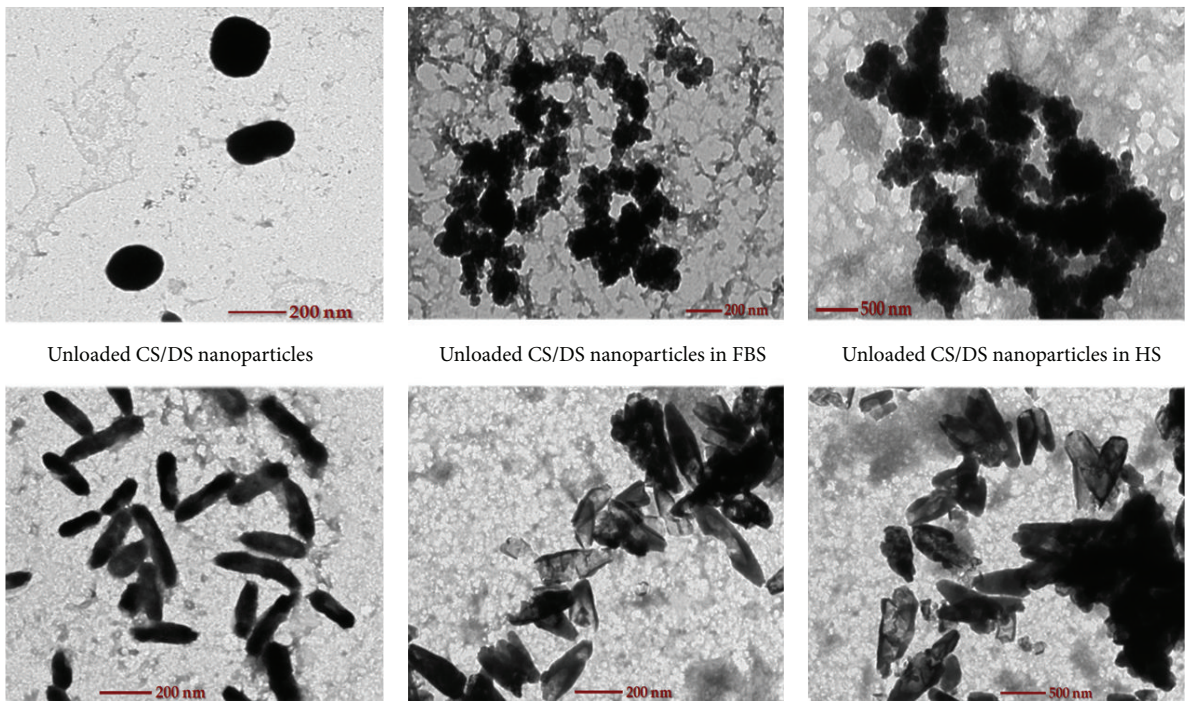

Figure 5: TEM micrographs of unloaded and BSA-loaded CS/DS nanoparticles before and at 24 h after incubation in human and fetal bovine sera. CS/DS nanoparticles were tend to form aggregates at 24 h after incubation in both FBS and HS (CS 0.075% w/v, BSA 1 mg/mL).

to swell by creating channels into the polymer. Thus, this promotes the penetration of medium between the forming molecules and results in higher swelling ratios. In contrast to that, the CS/DS nanoparticles with higher CS/DS weight ratios (1 : 1.7) have formed a compact infrastructure due to the stronger electrostatic interaction between $-NH_3^+$ groups of CS and $-SO_4^-$ groups donated by DS. The compact structure of nanoparticles will hinder the penetration of incubating medium into the polymer matrices and result in lesser extent of swelling. Lesser extent of swelling could also be explained by the fact that less cross-linking sites available on the surfaces of nanoparticles lead to lower interaction of polymer with water of hydration which did not allow the surrounded water to move inside the polymer channels and thus restrain the swelling of nanoparticles as shown in Figure 4.

Moreover, both unloaded and BSA-loaded nanoparticles had higher percent of swelling in HS as compared with FBS. The variation observed might be in response of varying interaction of nanoparticles with the different components of both sera. Despite that, it could be clearly seen that the unloaded CS/DS nanoparticles had higher swelling extent in both HS and FBS (Figure 4(a)) when compared with BSA-loaded CS/DS nanoparticles (Figure 4(b)). This could be explained on the basis that the BSA-loaded nanoparticles were presented in the swelling media with an extra barrier onto the surface of nanoparticles due to the loaded BSA molecules. This extra layer might prevent the diffusion of water of hydration into the polymer matrices and thus restrain the swelling of BSA-loaded nanoparticles as compared to unloaded one. Secondly, the BSA-loaded nanoparticles have lower cross-linking sites available to interact with surrounded water of hydration because of their lower surface charge caused by neutralization of loaded BSA molecules as compared to unloaded nanoparticles as previously discussed in Section 3.1.

3.4. Morphological Examination. The influence of FBS and HS on the morphology of incubating unloaded and BSA-loaded CS/DS nanoparticles was viewed under a TEM. The obtained TEM monograph of unloaded nanoparticles was observed to be smooth spheres before incubating in FBS or HS as shown in Figure 5(a). However, the results depict that the morphology of unloaded CS/DS nanoparticles was generally changed from smooth spheres to irregular one after incubating in FBS as shown in Figure 5(b). Similarly, Figure 5(c) revealed that the unloaded nanoparticles tend to form agglomerates at 24 h after incubation in HS. Taken together, the obtained monograph in Figure 5(c) clearly shows that the unloaded nanoparticles had a higher degree of irregularity as well as aggregation tendency in HS as compared with those incubated in FBS (Figure 5(b)). This finding was in accordance with the results of particle size which explained that the unloaded CS/DS nanoparticles did not show a significant increase in particle size when incubated in FBS at 24 h after incubation (~200 nm). In contrast to that, the particle size of unloaded nanoparticles was significantly

increased from ~200 to ~500 nm after incubating for 24 h in HS which could be clearly seen from Figure 5(c).

In addition, the morphology of BSA-loaded CS/DS nanoparticles (before incubation) was observed to be changed from smooth round-ended rod-shaped (Figure 5(a) bottom) to slight agglomeration after incubating in the FBS as shown in Figure 5(b) bottom. On the other hand, Figure 5(c) bottom shows that BSA-loaded NPs tend to form more compact and floccular aggregates when incubated in HS as compared to those incubated in FBS. Hence, the TEM micrographs clearly reveal that the HS imparts a more flocculating influence on the incubated CS/DS nanoparticles, regardless of unloaded one or BSA-loaded nanoparticles.

4. Conclusions

The present study was designed with the aim to explore the colloidal stability of unloaded and BSA-loaded CS/DS nanoparticles in FBS and HS. The results demonstrated that the BSA-loaded CS/DS nanoparticles had higher colloidal stability compared to the unloaded one in both FBS and HS. Moreover, the agglomeration extent of CS/DS nanoparticles was more pronounced in HS compared to FBS. Our findings therefore suggest that CS/DS nanoparticles were sufficiently stable in both serums.

Conflict of Interests

Authors report that there is no personal or financial conflict of interests in current research.

Acknowledgment

Authors gratefully acknowledge the "Dana Lonjakan Penerbitan" of Universiti Kebangsaan Malaysia (UKM-DLP-2011-001) for funding and supporting the current research project.

References

[1] K. Donaldson, X. Y. Li, and W. MacNee, "Ultrafine (nanometre) particle mediated lung injury," *Journal of Aerosol Science*, vol. 29, no. 5-6, pp. 553–560, 1998.

[2] G. Oberdorster, J. Ferin, R. Gelein, S. C. Soderholm, and J. Finkelstein, "Role of the alveolar macrophage in lung injury: studies with ultrafine particles," *Environmental Health Perspectives*, vol. 97, pp. 193–199, 1992.

[3] A. Nel, T. Xia, L. Madler, and N. Li, "Toxic potential of materials at the nano-level," *Science*, vol. 311, pp. 622–627, 2006.

[4] G. Oberdörster, E. Oberdörster, and J. Oberdörster, "An emerging discipline evolving from studies of ultrafine particles," *Environmental Health Perspectives*, vol. 113, pp. 823–839, 2005.

[5] J. M. Balbus, A. D. Maynard, V. L. Colvin et al., "Hazard assessment for nanoparticles: report from an interdisciplinary workshop," *Environmental Health Perspectives*, vol. 115, no. 11, pp. 1654–1659, 2007.

[6] I. Lynch, T. Cedervall, M. Lundqvist, C. Cabaleiro-Lago, S. Linse, and K. A. Dawson, "The nanoparticle-protein complex as a biological entity; a complex fluids and surface science challenge for the 21st century," *Advances in Colloid and Interface Science*, vol. 134-135, pp. 167–174, 2007.

[7] T. Cedervall, I. Lynch, S. Lindman et al., "Probing the interactions of proteins and nanoparticles," *Proceedings of the National Academy of Sciences of the United States of America*, vol. 104, no. 7, pp. 2029–2030, 2007.

[8] A. J. Vander, J. H. Sherman, and D. S. Luciano, *Human Physiology: The Mechanisms of Body Function*, McGraw-Hill, Boston, Mass, USA, 7th edition, 1998.

[9] J. van der Valk, D. Brunner, K. De Smet et al., "Optimization of chemically defined cell culture media—replacing fetal bovine serum in mammalian in vitro methods," *Toxicology In Vitro*, vol. 24, no. 4, pp. 1053–1063, 2010.

[10] N. Nafee, M. Schneider, U. F. Schaefer, and C. M. Lehr, "Relevance of the colloidal stability of chitosan/PLGA nanoparticles on their cytotoxicity profile," *International Journal of Pharmaceutics*, vol. 381, no. 2, pp. 130–139, 2009.

[11] O. Zelphati, L. S. Uyechi, L. G. Barron, and F. C. Szoka Jr., "Effect of serum components on the physico-chemical properties of cationic lipid/oligonucleotide complexes and on their interactions with cells," *Biochimica et Biophysica Acta*, vol. 1390, no. 2, pp. 119–133, 1998.

[12] L. Otvos Jr., C. Snyder, B. Condie, P. Bulet, and J. D. Wade, "Chimeric antimicrobial peptides exhibit multiple modes of action," *International Journal of Peptide Research and Therapeutics*, vol. 11, no. 1, pp. 29–42, 2005.

[13] M. J. Cooney, J. Petermann, C. Lau, and S. D. Minteer, "Characterization and evaluation of hydrophobically modified chitosan scaffolds: towards design of enzyme immobilized flow-through electrodes," *Carbohydrate Polymers*, vol. 75, no. 3, pp. 428–435, 2009.

[14] M. Peesan, P. Supaphol, and R. Rujiravanit, "Preparation and characterization of hexanoyl chitosan/polylactide blend films," *Carbohydrate Polymers*, vol. 60, no. 3, pp. 343–350, 2005.

[15] H. K. No, S. H. Kim, S. H. Lee, N. Y. Park, and W. Prinyawiwatkul, "Stability and antibacterial activity of chitosan solutions affected by storage temperature and time," *Carbohydydrate Polymers*, vol. 65, pp. 174–178, 2006.

[16] Q. Gan and T. Wang, "Chitosan nanoparticle as protein delivery carrier—systematic examination of fabrication conditions for efficient loading and release," *Colloids and Surfaces B*, vol. 59, no. 1, pp. 24–34, 2007.

[17] M. Rahimnejad, M. Jahanshahi, and G. D. Najafpour, "Production of biological nanoparticles from bovine serum albumin for drug delivery," *African Journal of Biotechnology*, vol. 5, no. 20, pp. 1918–1923, 2006.

[18] P. Calvo, C. Remunan, J. J. L. Vila, and M. J. Alonso, "Novel hydrophilic chitosan-polyethylene oxide nanoparticles as protein carriers," *Journal of Applied Polymer Science*, vol. 63, pp. 125–132, 1997.

[19] Y. Chen, V. J. Mohanraj, F. Wang, and H. A. E. Benson, "Designing chitosan-dextran sulphate nanoparticles using charge ratios," *AAPS Pharmaceutical Science and Technology*, vol. 8, pp. 131–139, 2007.

[20] R. H. Müller, S. Maaßen, H. Weyhers, and W. Mehnert, "Phagocytic uptake and cytotoxicity of solid lipid nanoparticles (SLN) sterically stabilized with poloxamine 908 and poloxamer 407," *Journal of Drug Targeting*, vol. 4, no. 3, pp. 161–170, 1996.

[21] H. Beatrice, P. Saulnier, B. Pech, J. E. Proust, and J. P. Benoit, "Physico-chemical stability of colloidal lipid particles," *Biomaterials*, vol. 24, pp. 4283–4300, 2003.

[22] S. Papadimitriou, D. Bikiaris, K. Avgoustakis, E. Karavas, and M. Georgarakis, "Chitosan nanoparticles loaded with dorzolamide and pramipexole," *Carbohydrate Polymers*, vol. 73, no. 1, pp. 44–54, 2008.

[23] E. Leo, C. Contado, F. Bortolotti et al., "Nanoparticle formulation may affect the stabilization of an antiischemic prodrug," *International Journal of Pharmaceutics*, vol. 307, no. 1, pp. 103–113, 2006.

[24] Y. Chen, V. J. Mohanraj, and J. E. Parkin, "Chitosan-dextran sulfate nanoparticles for delivery of an anti-angiogenesis peptide," *Letters in Peptide Science*, vol. 10, no. 5-6, pp. 621–629, 2003.

[25] M. G. Anhorn, M. Hanns-Christian, and K. Langer, "Pharmaceutical nanotechnology," *International Journal of Pharmaceutics*, vol. 363, pp. 162–169, 2008.

[26] P. Calvo, C. Remuñan-López, J. L. Vila-Jato, and M. J. Alonso, "Chitosan and chitosan/ethylene oxide-propylene oxide block copolymer nanoparticles as novel carriers for proteins and vaccines," *Pharmaceutical Research*, vol. 14, pp. 1431–1436, 1997.

[27] N. Fogh-Andersen, P. J. Bjerrum, and O. Siggaard-Andersen, "Ionic binding, net charge, and Donnan effect of human serum albumin as a function of pH," *Clinical Chemistry*, vol. 39, no. 1, pp. 48–52, 1993.

[28] J. Qi, P. Yao, F. He, C. Yu, and C. Huang, "Nanoparticles with dextran/chitosan shell and BSA/chitosan core—doxorubicin loading and delivery," *International Journal of Pharmaceutics*, vol. 393, no. 1-2, pp. 177–185, 2010.

[29] J. Dobson, "Gene therapy progress and prospects: magnetic nanoparticle-based gene delivery," *Gene Therapy*, vol. 13, no. 4, pp. 283–287, 2006.

[30] T. Blunk, M. Luck, A. Calvor et al., "Kinetics of plasma protein adsorption on model particles for controlled drug delivery and drug targeting," *European Journal of Pharmaceutics and Biopharmaceutics*, vol. 42, no. 4, pp. 262–268, 1996.

[31] T. M. Goppert and R. H. Muller, "Adsorption kinetics of plasma proteins on solid lipid nanoparticles for drug targeting," *International Journal of Pharmaceutics*, vol. 302, pp. 172–186, 2005.

[32] H. Katas, Z. Hussain, and T. C. Ling, "Chitosan nanoparticles as a percutaneous drug delivery system for hydrocortisone," *Journal of Nanomaterials*, vol. 2012, Article ID 372725, 11 pages, 2012.

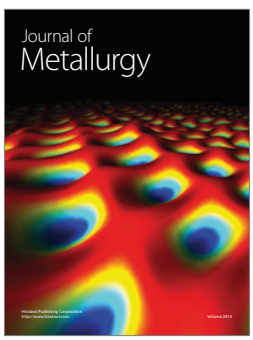

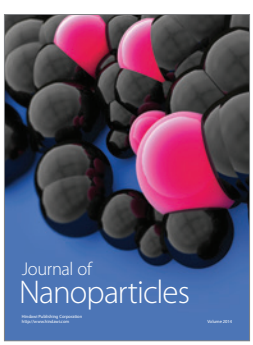

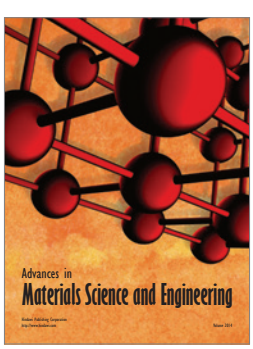

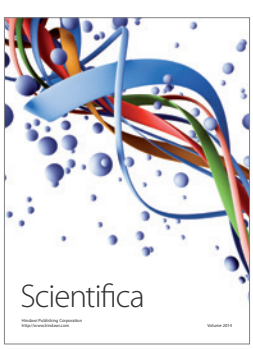

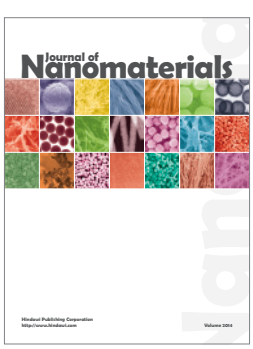

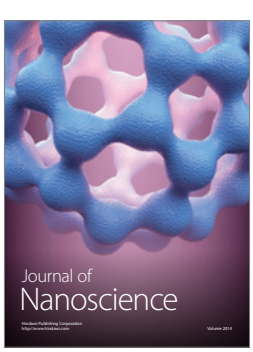

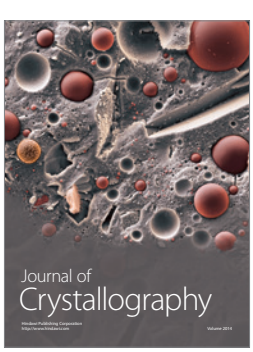

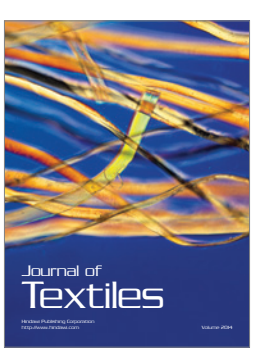

Hindawi

Submit your manuscripts at
http://www.hindawi.com